SEISMIC BEARING CAPACITY OF CIRCULAR FOOTINGS:
A YIELD DESIGN APPROACH

Jean Salençon, Charisis Theodorou Chatzigogos and Alain Pecker

SEISMIC BEARING CAPACITY OF CIRCULAR FOOTINGS: A YIELD DESIGN APPROACH

JEAN SALENÇON, CHARISIS THEODOROU CHATZIGOGOS AND ALAIN PECKER

As developed during the past decades, the yield design theory provides an approach to the stability analysis of civil engineering structures under seismic conditions which has been often used, explicitly or implicitly. New results related to circular footings resting on a purely cohesive soil, taking into account the horizontal inertia forces, are presented in this paper for practical applications to the safety coefficient to be applied to the vertical load when designing seismic foundations.

An outline of yield design theory

Just to clarify the terminology and to fix the notations, a brief outline of the yield design theory [Salençon 1983; 1990] is recalled here within the three dimensional continuum mechanics framework. It aims at estimating the *extreme loads* that can be supported by a structure from the knowledge of its geometry, of the loading process it undergoes and of the strength criteria of its constituent materials, whatever the physical phenomena they are related to. Since they do not refer to any data about the constitutive law of its materials before and at failure, the results obtained are but upper bound estimates for the *actual* ultimate loads and no information can be obtained regarding the displacements. With the generic notations Ω and $\partial\Omega$ for the volume and the boundary of the system, the quasistatic loading mode of the system is described through a multiparameter loading vector $\boldsymbol{Q}$ with components Q_i and the associated dual kinematic parameters $\hat{q}_i$ defining the virtual kinematic vector $\hat{\boldsymbol{q}}$. The principle of virtual rates of work [Salençon 2001] thus takes the form: *for all $\boldsymbol{\sigma}$ statically admissible with $\boldsymbol{Q}$, and all $\hat{\boldsymbol{U}}$ kinematically admissible with $\hat{\boldsymbol{q}}$,*

$$\int_{\Omega} \boldsymbol{\sigma} : \hat{\boldsymbol{d}} \, d\Omega + \int_{\Sigma_{\hat{U}}} \boldsymbol{n} \cdot \boldsymbol{\sigma} \cdot [\![\hat{\boldsymbol{U}}]\!] \, d\Sigma_{\hat{U}} = \boldsymbol{Q} \cdot \hat{\boldsymbol{q}}, \tag{1}$$

with

$$\boldsymbol{\sigma} \mapsto \boldsymbol{Q} \quad and \quad \hat{\boldsymbol{U}} \mapsto \hat{\boldsymbol{q}} \quad linear, \tag{2}$$

where the symbol ":" denotes the double contracted product and "·" the dot product. $\boldsymbol{\sigma}$ stands for the Cauchy stress tensor field, and $\hat{\boldsymbol{d}}$ for the virtual strain rate tensor field derived from the virtual velocity field $\hat{\boldsymbol{U}}$. Since such a field may exhibit velocity jumps $[\![\hat{\boldsymbol{U}}]\!]$ across velocity jump surfaces $\Sigma_{\hat{U}}$ which are part of its definition, the second term in Equation (1) accounts for the corresponding contribution.

The same description is adopted in the case of a dynamic loading treated as a quasistatic phenomenon by incorporating the corresponding given inertia forces within the applied external forces.

Homogeneity is not assumed and the term *constituent material* will be used generically from now on to describe all the materials constituting the system, including the interfaces between different elements.

The resistance of the constituent material is defined at any point of the system through a convex strength criterion to be satisfied by the stress state.

When trying to determine the loads $\boldsymbol{Q}$ that can be supported by the system under the specified strength conditions, it is clear that mathematical compatibility at any point of the system between the equilibrium equations and the material resistance conditions is necessary for a load to be supported. Such loads generate the convex domain of the *potentially safe* loads in the $\boldsymbol{Q}$ vector space. The boundary of K defines the *extreme loads* of the system. Any stress field in equilibrium with a load $\boldsymbol{Q}$ that complies with the strength criterion is sufficient to prove that $\boldsymbol{Q} \in K$. This is the basis of the *internal approach* or lower bound approach to the extreme loads. Although the extreme loads are but upper bound estimates of the actual ultimate loads of the system, it must be emphasized that since they are independent of the material behaviour characteristics, other than the strength criteria, and of the loading paths and loading history, they are valid regardless of these data. Thus, after being assessed and through the introduction of convenient safety factors, they provide a reliable theoretical benchmark for practical applications.

The construction of stress fields that satisfy the conditions above often makes the implementation of the internal approach difficult. Dualization through the principle of virtual rates of work (see Equations (1) and (2)) leads to an external approach based upon the construction of kinematically admissible virtual velocity fields. The details of the related reasoning can be found in [Salençon 1990]. The key idea is that the material resistance may be equivalently defined through the strength criteria on the stress tensor, as indicated above, or through the associated π-functions of the strain rate $\hat{\boldsymbol{d}}$: denoting generically by G the domain of resistance on $\boldsymbol{\sigma}$ defined at a point of the system, the corresponding π-function is just the *support function*

$$\pi(\hat{\boldsymbol{d}}) = \sup\{\boldsymbol{\sigma}' : \hat{\boldsymbol{d}} \mid \boldsymbol{\sigma}' \in G\}, \tag{3}$$

from which we derive

$$\pi(\boldsymbol{n}, [\![\hat{\boldsymbol{U}}]\!]) = \sup\{\boldsymbol{n} \cdot \boldsymbol{\sigma}' \cdot [\![\hat{\boldsymbol{U}}]\!] \mid \boldsymbol{\sigma}' \in G\}. \tag{4}$$

The π-functions are called the maximum resisting rate of work densities related to G. From the definition of K and through Equations (1) and (2), the fundamental inequality of the external approach is obtained in the form: For every $\boldsymbol{Q} \in K$, and every kinematically admissible virtual velocity field $\hat{\boldsymbol{U}}$,

$$\boldsymbol{Q} \cdot \hat{\boldsymbol{q}} \leq \int_{\Omega} \pi(\hat{\boldsymbol{d}}) \, d\Omega + \int_{\Sigma_{\hat{U}}} \pi(\boldsymbol{n}, [\![\hat{\boldsymbol{U}}]\!]) \, d\Sigma_{\hat{U}}. \tag{5}$$

The right side of Equation (5) is called the maximum resisting rate of work in the virtual velocity field $\hat{\boldsymbol{U}}$:

$$P_{\mathrm{rm}}(\hat{\boldsymbol{U}}) = \int_{\Omega} \pi(\hat{\boldsymbol{d}}) \, d\Omega + \int_{\Sigma_{\hat{U}}} \pi(\boldsymbol{n}, [\![\hat{\boldsymbol{U}}]\!]) \, d\Sigma_{\hat{U}}, \tag{6}$$

while the left side of (5) is just the rate of work of all the external forces $P_{\mathrm{e}}(\boldsymbol{Q}, \hat{\boldsymbol{U}})$. It follows from Equations (5) and (6) that the construction of any kinematically admissible virtual velocity field yields an external approximation of the boundary of K:

$$K \subset \{P_{\mathrm{e}}(\boldsymbol{Q}, \hat{\boldsymbol{U}}) - P_{\mathrm{rm}}(\hat{\boldsymbol{U}}) \leq 0\}, \quad \text{for any kinematically admissible } \hat{\boldsymbol{U}}. \tag{7}$$
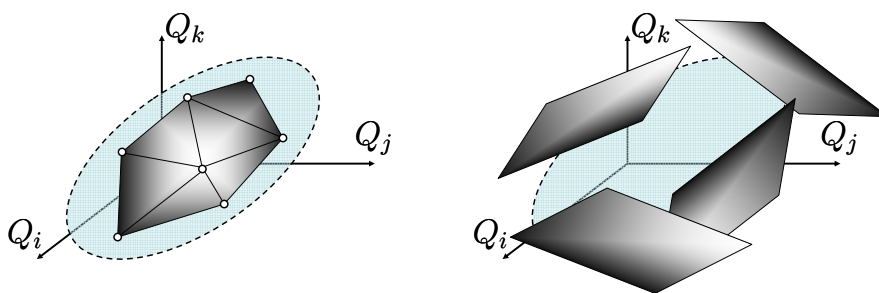
Figure 1. Internal and external approaches to the domain of potentially safe loads.

The two approaches are schematically presented in Figure 1. Important points regarding the external approach are:

- Tables giving the expressions of the π-functions for usually encountered criteria are available [Salençon 1983; 2002].

- For a given G the values of the π-functions are either finite or infinite depending on the values of the arguments $\hat{\boldsymbol{d}}$ and $(\boldsymbol{n}, [\![\hat{\boldsymbol{U}}]\!])$.

- For the approach to be efficient, kinematically admissible virtual velocity fields $\hat{\boldsymbol{U}}$ must be chosen in order that the values of the π-functions remain finite everywhere in O.

- The third condition has no relationship whatsoever with a constitutive law.

One may wonder how the external approach can be of any use in practical applications for the design of structures since it only provides upper bounds of the extreme loads, the practical significance of which has been discussed above. As a matter of fact, this is one reason for the introduction of the *model factor* in ultimate limit state design codes [Salençon 1994]. Independently of the partial safety factors which define the design loads and design resistances to be introduced in the design procedure of the considered structure, derived from the nominal ones, the model factor is imposed on the resisting rate of work as a whole in order to take into account the method for the yield design analysis that is performed (say, by assessing the *quality* of the considered potential collapse mechanisms).

Seismic bearing capacity of a circular footing on a purely cohesive soil

Problem motivation. The problem under consideration arises from a series of field observations after several major earthquakes within the last twenty-five years, which revealed a particular type of foundation failure without the presence of liquefaction in the supporting soil layers: large permanent rotations were observed at the foundation level together with a zone of detachment at the soil-foundation interface and the development of a failure mechanism within the soil volume [Mendoza and Auvinet 1988]. The same failure mechanism was also identified experimentally [Knappett et al. 2006; Zeng and Steedman 1998].

From a theoretical point of view, one initial approach to the problem of the seismic bearing capacity is to work within the classical framework of Terzaghi's bearing capacity formula, modifying the bearing capacity factors in order to account for the effect of the inertia forces within the soil volume during the seismic excitation, while applying appropriate correction factors for the load eccentricity and inclination

[Fishman et al. 2003; Richards et al. 1993; Sarma and Iossifelis 1990]. A second approach represents the seismic bearing capacity of the foundation system as an *ultimate surface* in the space of the loading parameters of the footing as a function of the intensity of the horizontal inertia forces in the soil volume [Paolucci and Pecker 1997a; 1997b; Pecker and Salençon 1991; Salençon and Pecker 1995a; 1995b]. The results so obtained in the case of shallow strip footings were incorporated in the European norms for earthquake-resistant design of civil engineering structures [Eurocode 1998].

This study aims at extending the analysis to the seismic bearing capacity of a shallow circular footing resting on the surface of a purely cohesive soil layer.

Definition of the seismic bearing capacity problem. A rigid circular footing with radius r resting on a purely cohesive soil half-space is considered (Figure 2). The resistance of the constituent soil is described by the Tresca criterion with a cohesion c depending linearly on the depth (8), with c_0 being the surface cohesion and α the vertical cohesion gradient:

$$c = c_0 = \alpha z. \tag{8}$$

In order to assess the importance of the corresponding assumption, two extreme cases are considered, namely, the classical Tresca criterion (9) and the Tresca criterion with zero resistance to tension (10):

$$f(\boldsymbol{\sigma}) = |\sigma_1 - \sigma_3| - 2c \le 0, \tag{9}$$

$$f(\boldsymbol{\sigma}) = \sup\{|\sigma_1 - \sigma_3| - 2c, \sigma_1\} \le 0, \tag{10}$$

with σ_1 and σ_3 being the major and minor principal stresses respectively (tensile stresses positive).

The soil-footing interface is also considered to be purely cohesive and its resistance is modelled by the Tresca criterion with no tensile resistance (zero tension *cut-off*). This is a deliberate choice in order to allow for the potential creation of a zone of detachment between the footing and the soil, an essential characteristic of observed seismic bearing capacity failure. The interface cohesion is considered equal to c_0.

$$f(\sigma, \tau) = \sup\{|\tau| - c_0, \sigma\} \le 0. \tag{11}$$

The quasistatic loading mode of the system is defined by means of the wrench of external forces acting on the footing due to the weight and to the inertial response of the superstructure (including the footing itself), of the unit weight of the soil, and of the intensity of the inertia forces developing within the soil mass.

Following common practice, this intensity is assumed to be uniform throughout the soil mass with vertical and horizontal components F_v and F_h. The physical validity of this assumption has already been discussed by various authors (for example, Pecker and Salençon [1991] suggested that, denoting by d
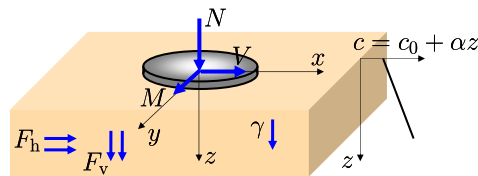

Figure 2. Circular shallow foundation under seismic loading on a purely cohesive soil.

and D the failure mechanism thickness and the depth of the soil layer, the following condition should be satisfied: $d/D < 10$) and will be revisited in a following section. From now on the vertical component will be added to the unit weight of the soil and will give rise to the modified unit weight:

$$\boldsymbol{\gamma}^* = \boldsymbol{\gamma} + \boldsymbol{F}_{\mathrm{v}} = \gamma^* \boldsymbol{e}_z, \tag{12}$$

with $\boldsymbol{e}_z$ the unit vector in the descending vertical direction.

Due to the origin of the external loads acting on the superstructure and on the foundation, it is also assumed that the horizontal component V of the resultant force of the wrench is collinear with the horizontal inertia force F_{h} in the soil along the x-axis, and that the horizontal overturning moment M at the center of the footing is oriented around the y-axis, perpendicular to that direction. As a matter of fact, this assumption is rigorously valid when dealing with the excitation of a single-degree-of-freedom (SDOF) superstructure and under specific conditions in the case of multiple degrees of freedom.

Relevant variables for the seismic bearing capacity problem. The determination of the bearing capacity of the foundation under the conditions specified above is based upon the theory of yield design. Concerning the influence of the modified unit weight on the extreme loads, it has been shown [Salençon 1983] that, for the classical Tresca criterion, the unit weight has no influence on the value of the extreme loads supported by the footing. The result holds also if the modified unit weight is not constant but depends only on the z-coordinate. For the case of the Tresca criterion with no resistance to tension, the result remains true if $\gamma^* \leq 0$, which is true in the usual cases of seismic excitations. Therefore, γ^* will no longer appear in the problem loading parameters.

Dimensionless parameters. The vertical component of the resultant force acting on the footing is denoted by N. The horizontal component F_{h} is defined from a horizontal acceleration a_{h} characteristic of the examined earthquake, which can be for instance the peak ground horizontal acceleration (PGHA):

$$F_{\mathrm{h}} = \rho a_{\mathrm{h}}, \tag{13}$$

with ρ being the mass density of the soil.

The vector $\boldsymbol{Q}$ representing the loading parameters of the system is written as

$$\boldsymbol{Q} = (N, V, M, F_{\mathrm{h}}), \tag{14}$$

and the strength parameters are c_0 and α.

When presenting the results, dimensionless parameters will be introduced:

$$\tilde{N} = \frac{N}{\pi c_0 r^2}, \quad \tilde{V} = \frac{V}{\pi c_0 r^2}, \quad \tilde{M} = \frac{M}{2\pi c_0 r^3}, \quad \tilde{F}_{\mathrm{h}} = \frac{\rho r a_{\mathrm{h}}}{\pi c_0}, \quad \tilde{k} = \frac{r\alpha}{c_0}. \tag{15}$$

The parameter $\tilde{k}$ expresses the degree of heterogeneity in the system. For a homogeneous soil layer, $\tilde{k} = 0$. Common values of r, α and c_0 give rise to $\tilde{k}$ less than or equal to approximately 2.

Solution procedure. The external approach is implemented in this problem through the construction of kinematically admissible virtual velocity fields in the whole system that are relevant to the strength criteria under consideration by referring to the π-functions corresponding to Equations (9)–(11):

- Classical Tresca criterion (Equation (9)):

$$
\begin{aligned}
\pi(\hat{\boldsymbol{d}}) &= +\infty && \text{if } \operatorname{tr}(\hat{\boldsymbol{d}}) \neq 0, \\
\pi(\hat{\boldsymbol{d}}) &= c(|\hat{d}_1| + |\hat{d}_2| + |\hat{d}_3|) && \text{if } \operatorname{tr}(\hat{\boldsymbol{d}}) = 0, \\
\pi(\boldsymbol{n}, [\![\hat{\boldsymbol{U}}]\!]) &= +\infty && \text{if } [\![\hat{\boldsymbol{U}}]\!] \cdot \boldsymbol{n} \neq 0, \\
\pi(\boldsymbol{n}, [\![\hat{\boldsymbol{U}}]\!]) &= c|[\![\hat{\boldsymbol{U}}]\!]| && \text{if } [\![\hat{\boldsymbol{U}}]\!] \cdot \boldsymbol{n} = 0.
\end{aligned}
\tag{16}
$$

- Tresca criterion with zero tension cut-off (Equation (10)):

$$
\begin{aligned}
\pi(\hat{\boldsymbol{d}}) &= +\infty && \text{if } \operatorname{tr}(\hat{\boldsymbol{d}}) < 0, \\
\pi(\hat{\boldsymbol{d}}) &= c(|\hat{d}_1| + |\hat{d}_2| + |\hat{d}_3| - \operatorname{tr}(\hat{\boldsymbol{d}})) && \text{if } \operatorname{tr}(\hat{\boldsymbol{d}}) \geq 0, \\
\pi(\boldsymbol{n}, [\![\hat{\boldsymbol{U}}]\!]) &= +\infty && \text{if } [\![\hat{\boldsymbol{U}}]\!] \cdot \boldsymbol{n} < 0, \\
\pi(\boldsymbol{n}, [\![\hat{\boldsymbol{U}}]\!]) &= c|[\![\hat{\boldsymbol{U}}]\!] - [\![\hat{\boldsymbol{U}}]\!] \cdot \boldsymbol{n}| && \text{if } [\![\hat{\boldsymbol{U}}]\!] \cdot \boldsymbol{n} \geq 0.
\end{aligned}
\tag{17}
$$

- Tresca criterion for the interface without resistance to tension (Equation (11)):

$$
\begin{aligned}
\pi(\boldsymbol{n}, [\![\hat{\boldsymbol{U}}]\!]) &= +\infty && \text{if } [\![\hat{\boldsymbol{U}}]\!] \cdot \boldsymbol{n} < 0, \\
\pi(\boldsymbol{n}, [\![\hat{\boldsymbol{U}}]\!]) &= c|[\![\hat{\boldsymbol{U}}]\!] - ([\![\hat{\boldsymbol{U}}]\!] \cdot \boldsymbol{n}) \cdot \boldsymbol{n}| && \text{if } [\![\hat{\boldsymbol{U}}]\!] \cdot \boldsymbol{n} \geq 0.
\end{aligned}
\tag{18}
$$

It follows obviously that a relevant virtual velocity field for the classical Tresca criterion is also relevant for the Tresca criterion without tensile strength, but not vice versa. Attention must be paid also to Equation (18) as it shows that a nonzero maximum resisting rate of work is obtained even when a detachment between the footing and the soil is induced by the virtual velocity field.

Since the circular footing is assumed to be perfectly rigid, any kinematically admissible virtual velocity $\hat{\boldsymbol{U}}$ field must comply with a rigid body motion of the footing as a boundary condition. For the planar velocity fields that will be considered hereafter, assuming $\hat{U}_y = 0$, such a rigid body motion is defined by the virtual rate of rotation $\hat{\omega}$ and the two components $\hat{U}_{O,x}$, $\hat{U}_{O,z}$ of the virtual velocity of the center O of the footing. Consequently the rate of work of the external forces is written:

$$
\boldsymbol{Q} \cdot \hat{\dot{\boldsymbol{q}}} = N\hat{U}_{O,z} + V\hat{U}_{O,x} + M\hat{\omega} + F_{\mathrm{h}} \int_{\Omega} \hat{\boldsymbol{U}} \cdot \boldsymbol{e_x} \, dO.
\tag{19}
$$

Three classes of kinematically admissible virtual velocity fields $\hat{\boldsymbol{U}}$ have been examined, which are derived from plane strain potential failure mechanisms used to determine the seismic bearing capacity of strip footings. Completely described in [Chatzigogos 2007; Chatzigogos et al. 2007], these planar and nonplane strain virtual velocity fields are parallel to Oxz and depend on the three coordinates. They are relevant to the strength criteria (Equations (9)–(11)) since they are isochoric everywhere in Ω: $\operatorname{tr}(\hat{\boldsymbol{d}}) = 0$, $[\![\hat{\boldsymbol{U}}]\!] \cdot \boldsymbol{n} = 0$, but for the interface where virtual uplift of the footing with respect to the soil surface may occur $[\![\hat{\boldsymbol{U}}]\!] \cdot \boldsymbol{n} \geq 0$. In order to implement the external approach through Equation (7) $P_{\mathrm{rm}}(\hat{\boldsymbol{U}})$ must be computed, which implies deriving $\hat{\boldsymbol{d}}$ from $\hat{\boldsymbol{U}}$, a tedious task until it was drastically simplified by Puzrin and Randolph [2003a; 2003b] in a method based upon the use of wisely chosen curvilinear coordinates.

- *Translational* virtual failure mechanisms were originally proposed in plane strain [Green 1954] for the indentation by a rigid punch submitted to an inclined load; the extension to a rigid circular footing was given by Puzrin and Randolph [2003b] by considering that the width of the mechanism in a cross-section by a vertical plane is proportional to the width of the footing in the same cross-section (Figure 3). The footing translates with a virtual velocity $\hat{U}_0$ which propagates with a constant magnitude along the streamlines of the mechanism. The shape of each virtual failure mechanism is defined by two angles: $0 < \delta < \pi/2$, $0 < \epsilon < \pi/2$. The mechanisms exhibit three zones within the soil mass, presented in Figure 3. Zones 1 and 3 translate rigidly while zone 2 is a region where nonplane shear strain rate is developed. Contributions to the maximum resisting rate of work for this class are developed within the volume of zone 2 and along the velocity jump surface in the soil. These virtual mechanisms involve no rotation of the footing: the upper bound estimates they provide through (7) do not involve the moment M.

- *Purely rotational* virtual failure mechanisms are adapted from the plane strain version studied in [Salençon and Pecker 1995a; 1995b; Sekiguchi and Kobayashi 1997]. The rigid circular footing is considered to rotate rigidly around an axis parallel to Oy and induces rigid rotational failure of the soil below with a virtual angular velocity $\hat{\omega}$ (Figure 4). Each mechanism is defined by the geometrical parameters κ and λ. For $1 < \lambda < 2$, there is no uplift of the footing with respect to the soil surface and the maximum resisting rate of work is only produced along the velocity jump surface within the soil volume. For $0 < \lambda < 1$, uplift of the footing with respect to the soil surface takes place in the zone of soil-footing detachment where consequently a fraction of the maximum resisting rate of work is developed.

- *Shear-rotational* virtual failure mechanisms follow a pattern derived from the plane-strain virtual velocity field originally proposed by Hansen [1953] for the study of active earth pressures (see Figure 5).
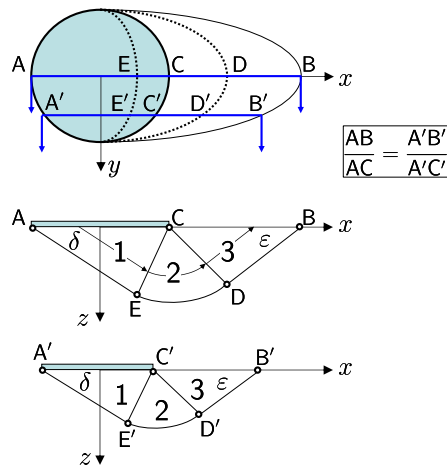

Figure 3. Translational virtual failure mechanism.
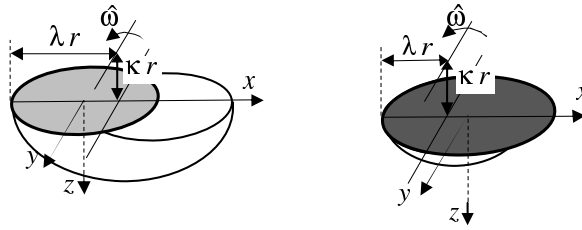
Figure 4. Purely rotational virtual failure mechanism.

Rigid body rotation of the footing around an axis of rotation parallel to Oy located within the soil mass induces the development of nonplanar shear strain rate in the zones 2 and 3 within the soil volume. The mechanisms depend on the three geometrical parameters κ, λ, μ and three distinct configurations are obtained depending on the position of the axis of rotation with respect to the footing: without uplift of the footing with respect to the soil surface or with a small or large zone of detachment; contributions to the maximum resisting rate of work are developed within the soil volume in zones 2 and 3, along the velocity jump surface in the soil mass and on the zone of soil-footing detachment, if any.

Results

Implementing the external approach through Equation (7), the rate of work of the external forces is given by (19) and the maximum resisting rate of work $P_{\mathrm{rm}}(\hat{U})$ is computed through (6) with the relevant expressions for $\pi(\hat{d})$ and $\pi(n, [\![\hat{U}]\!])$. Looking for optimal upper bounds for the ultimate loads supported by the system requires the implementation of an optimization procedure over each separate geometrical configuration of the three considered classes of virtual mechanisms: in each case, the mathematical problem involved reduces to minimizing a nonlinear objective function with respect to the parameters of the geometric configuration. The algorithm used for this purpose is described in [Coleman and Li 1996]. The following results were obtained.
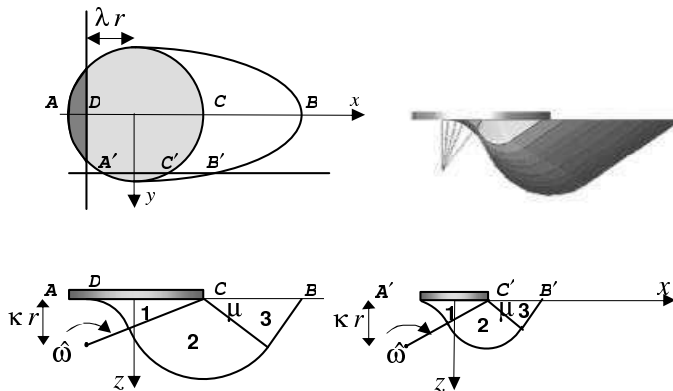

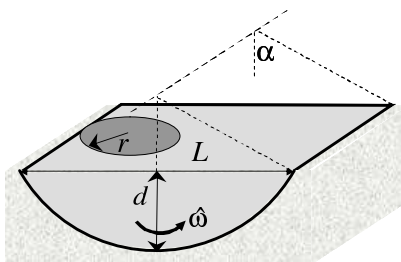**Figure 5.** Shear-rotational virtual failure mechanism.

Figure 6. Plane strain circular rigid body virtual collapse mechanism.

Critical value of F_h. The assumption of uniformly distributed horizontal inertia forces F_h would lead to a pathological conclusion if, in addition to the limitation on the ratio d/D which has already been introduced for physical relevance, the virtual failure mechanisms to be taken in consideration were given the possibility of infinite extension.

As an illustrative example, the plane strain circular rigid body virtual collapse mechanism presented in Figure 6 can be considered. In the case of a homogeneous soil layer, denoting by L and d its horizontal and vertical extension respectively, the minimization procedure on this class of mechanisms proves the instability of the system just due to the action of the soil inertia forces if $\rho a_h > 8.3 c_0/L = 2.74 c_0/d$, with the other loading parameters being zero: $\tilde{N} = 0$, $\tilde{V} = 0$, $\tilde{M} = 0$. As a consequence, for any circular footing with radius $r \leq L/2$, the value $\tilde{F}_h = 2.64 r/L = 0.87 d/L$ would appear as the critical value for the considered mechanism. This critical value tends to zero if the extension of the mechanism is unlimited. The value $\tilde{F}_h = 0$ would therefore appear as the critical value of $\tilde{F}_h$, a conclusion that is obviously unrealistic! This brings us to the condition that the virtual failure mechanisms implemented in the yield design theory must be physically relevant, apart from the fact that horizontal uniformity of $\tilde{F}_h$ could also be questioned. In other words, pathological circumstances are put aside through realistic constraints on the minimization procedure on the virtual failure mechanisms.

Table 1 summarizes the calculated values of critical $\tilde{F}_h$ as a function of $\tilde{k}$ for the three classes of examined three-dimensional virtual failure mechanisms. As could be anticipated, it shows that the critical value increases with $\tilde{k}$. The minimum value is obtained for the homogeneous soil ($\tilde{k} = 0$) through a shear-rotational virtual failure mechanism. For usual values of the other parameters such as $r = 4$ m, $c_0 = 20$ kPa, $\rho = 2 \times 10^3$ kg/m^3 it corresponds to a very strong earthquake: $a_h = 5$ m/sec$^2 \cong 0.5g$.

Class of mechanisms	Critical value of $\tilde{F}_h$			
	$\tilde{k} = 0$	$\tilde{k} = 0.5$	$\tilde{k} = 1$	$\tilde{k} = 3$
Translational	1.32	1.80	2.29	4.05
Purely rotational	0.99	1.28	1.54	2.45
Shear rotational	0.66	0.90	1.15	2.03
MINIMUM	0.66	0.90	1.15	2.03

Table 1. Critical values of $\tilde{F}_h$ as a function of $\tilde{k}$.
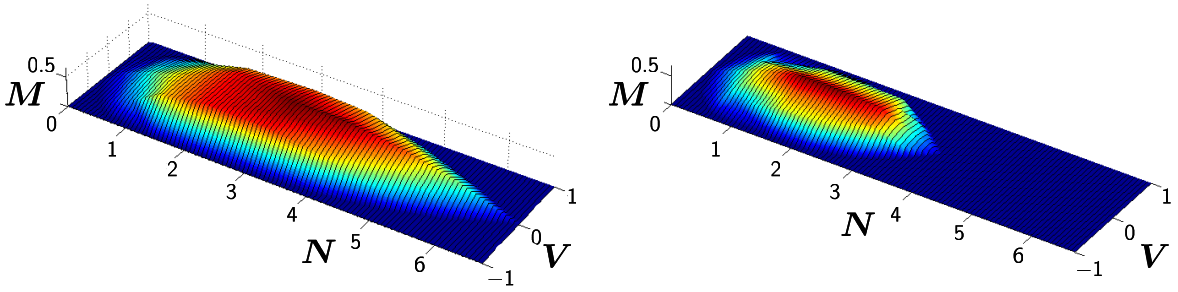
Figure 7. External approach of the ultimate load surface for a homogeneous soil ($\tilde{k} = 0$) when $\tilde{F}_\mathrm{h} = 0$ (left) and $\tilde{F}_\mathrm{h} = 0.5$ (right).

Presentation of the results. The upper bounds for the ultimate loads supported by the foundation are represented as surfaces in the space of the loading parameters ($\tilde{N}$, $\tilde{V}$, $\tilde{M}$) for different values of $\tilde{F}_\mathrm{h}$ and $\tilde{k}$ (Figure 7).

Since these surfaces are obtained through the minimization procedure described earlier over three different classes of virtual collapse mechanisms, they are just piecewise regular, each smooth part being the result of one class of mechanisms as it will appear in the interaction diagrams (Figures 8–9).

For practical applications the most convenient presentation of the results is by means of sections of those surfaces that may be called classically *interaction diagrams*: these curves represent the upper bounds for the ultimate combinations of the loading parameters and indicate the class of mechanisms from which each bound is obtained. In the following, the results refer to the Tresca criterion with a zero tension cut-off for the soil strength which seems the most realistic criterion to be considered. For brevity's sake, only some significant results will be reported here; a comprehensive and commented report may be found in [Chatzigogos 2007; Chatzigogos et al. 2007].

Interaction diagram ($\tilde{N}$, $\tilde{V}$, $\tilde{M} = 0$, $\tilde{F}_\mathrm{h}$). The diagrams in Figure 8 present the relation between the ultimate horizontal and vertical force for $\tilde{k} = 0$ and $\tilde{k} = 1$, for three different values of $\tilde{F}_\mathrm{h}$. The maximum value for $\tilde{V}$ is 1, corresponding to a translational mechanism of failure by pure sliding along the soil-footing interface when $\tilde{F}_\mathrm{h} = 0$. It is also interesting to note that for $\tilde{F}_\mathrm{h} > 0$ the purely rotational virtual mechanism gives an upper bound that is slightly better than the pure sliding one: although the depth of this mechanism is relatively small, so that it is very close to a pure sliding, it incorporates a contribution of $\tilde{F}_\mathrm{h}$ to the rate of work of the external forces. This phenomenon is less pronounced for larger values of $\tilde{k}$ as revealed by the diagram for $k = 1$. For practical applications it is worth noting that, both for $\tilde{k} = 0$ and for $\tilde{k} = 1$, the effect of $\tilde{F}_\mathrm{h}$ remains negligible as long as $\tilde{N}^0_\mathrm{max}/\tilde{N} > 2.5$, where $\tilde{N}^0_\mathrm{max}$ denotes the known exact value of the maximal vertical force supported by the footing with $\tilde{F}_\mathrm{h} = 0$ [Salençon and Matar 1982]. As $\tilde{N}$ increases so does the negative effect of a high value of $\tilde{F}_\mathrm{h}$, especially when $\tilde{N}^0_\mathrm{max}/\tilde{N} > 2i$ but it is observed that it is less pronounced for $\tilde{k} = 0$ than for $\tilde{k} = 1$: a favourable effect of the vertical cohesion gradient.

Interaction diagram ($\tilde{N}$, $\tilde{V}$, $\tilde{M} = 0$, $\tilde{F}_\mathrm{h}$). Figure 10 presents the optimal upper bounds for the ultimate combinations of $\tilde{M}$ and $\tilde{N}$ obtained with $\tilde{V} = 0$, for $\tilde{k} = 0$ and $\tilde{k} = 1$. Experimental data in the case $\tilde{k} = 0$, $\tilde{F}_\mathrm{h} = 0$ in [Houlsby and Martin 1993] are plotted for comparison.
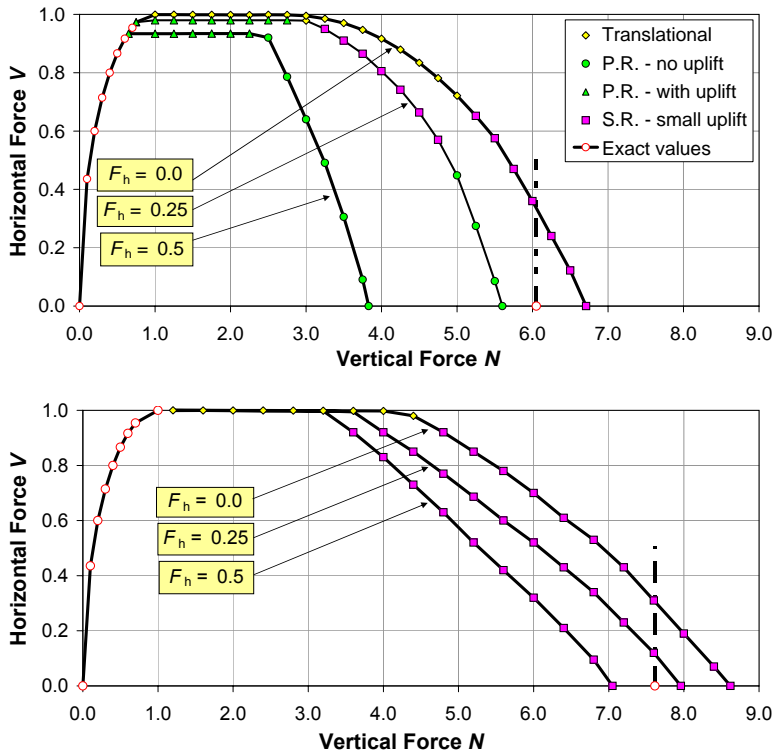
Figure 8. Interaction diagram ($\tilde{N}$, $\tilde{V}$, $\tilde{M} = 0$, $\tilde{F}_h$) for $\tilde{k} = 0$ (top) and $\tilde{k} = 1$ (bottom). Tresca criterion with zero tension cut-off.

It comes out that the upper bounds are satisfactory, from a practical point of view, and that the difference is larger for the larger values of $\tilde{N}$ that correspond to quasiaxisymmetric loading configurations, to which the considered unilateral virtual failure mechanisms are not well suited. For small values of $\tilde{N}$, the optimal upper bounds are obtained by mechanisms with a significant zone of detachment of the footing, which is not the case as $\tilde{N}$ increases. The effect of $\tilde{F}_h$ follows the same behaviour as in Figure 8, which, from a practical point of view, enforces the conclusion from this observation that a factor of safety against permanent loads $\tilde{N}_{max}^0 / \tilde{N} > 2.5$ can guarantee that the effect of soil inertia forces is negligible, even for very strong earthquakes. Such conclusions are in agreement with observations of real foundation bearing capacity failures, mainly after the Guerrero–Michoacán earthquake (Mexico, 1985) as presented in [Mendoza and Auvinet 1988].

Interaction diagram ($\tilde{N} = $ const, $\tilde{V}$, $\tilde{M}$, $\tilde{F}_h$). The interaction diagrams between the ultimate values of $\tilde{V}$ and $\tilde{M}$ for fixed values of the vertical force $\tilde{N}$ are shown in Figure 9 for $\tilde{k} = 0$ in the two cases $\tilde{N}_{max}^0 / \tilde{N} = 3$ corresponding to a proper foundation design and $\tilde{N}_{max}^0 / \tilde{N} = 1.5$ corresponding to a nonconservative design.

These diagrams can be used for practical applications when a relationship between the resultant moment and the horizontal force (base shear force) on the footing is known from the geometrical and
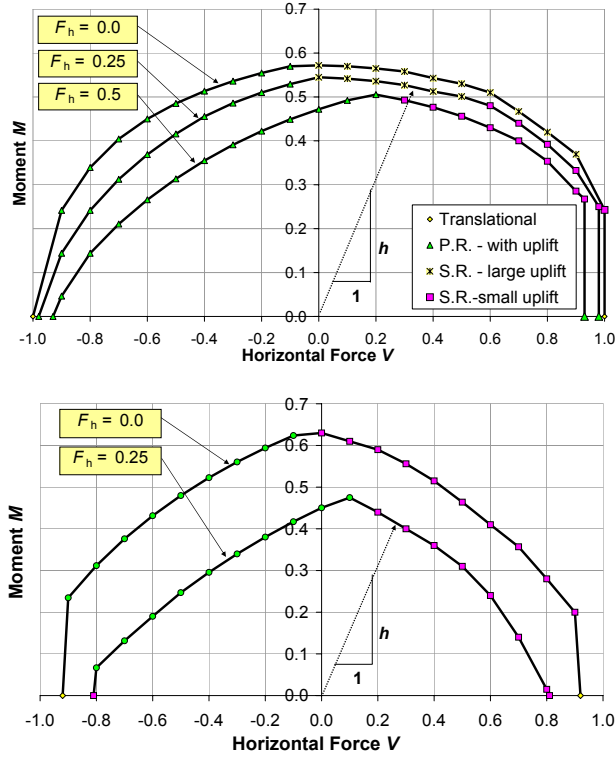
Figure 9. Tresca criterion with zero tension cut-off: interaction diagram ($\tilde{N}$ = const, $\tilde{V}$, $\tilde{M}$, $\tilde{F}_h$) for $\tilde{k} = 0$, $\tilde{N}^0_{\max}/\tilde{N} > 3$ (top) and $\tilde{N}^0_{\max}/\tilde{N} > 1.5$ (bottom); ultimate loading paths for $\tilde{F}_h = 0.25$ in a SDOF superstructure.

rigidity characteristics of the superstructure. Such a relationship defines a loading path in the ($\tilde{V}$, $\tilde{M}$)-plane allowing for the determination of the ultimate combination of $\tilde{V}$ and $\tilde{M}$ for given $\tilde{N}$ and $\tilde{F}_h$ as presented in Figure 10, it being observed that only the right halves of the diagrams, $\tilde{V} \geq 0$, correspond to realistic loading paths. The two diagrams highlight the significant decrease of the bearing capacity with increasing $\tilde{F}_h$ for $\tilde{N}^0_{\max}/\tilde{N} = 1.5$. Even for $\tilde{V} = 0$, $\tilde{M} = 0$, a value of $\tilde{F}_h = 0.5$ causes the collapse of the footing.

Practical implementation. As explained earlier, the Eurocode [1998] expression for the seismic bearing capacity of shallow foundations is only valid for strip footings resting on homogeneous soils, either purely cohesive or purely frictional. This study makes it possible to propose a modified version of those rules for shallow circular footings on a purely cohesive soil with a vertical cohesion gradient. The corresponding expression is presented and discussed in [Chatzigogos 2007; Chatzigogos et al. 2007]. As far as the design principles are concerned, it should be remembered that the effect of the horizontal inertia forces in the soil volume is, in general, negligible as long as the vertical force on the footing remains smaller than one third of its static bearing capacity.
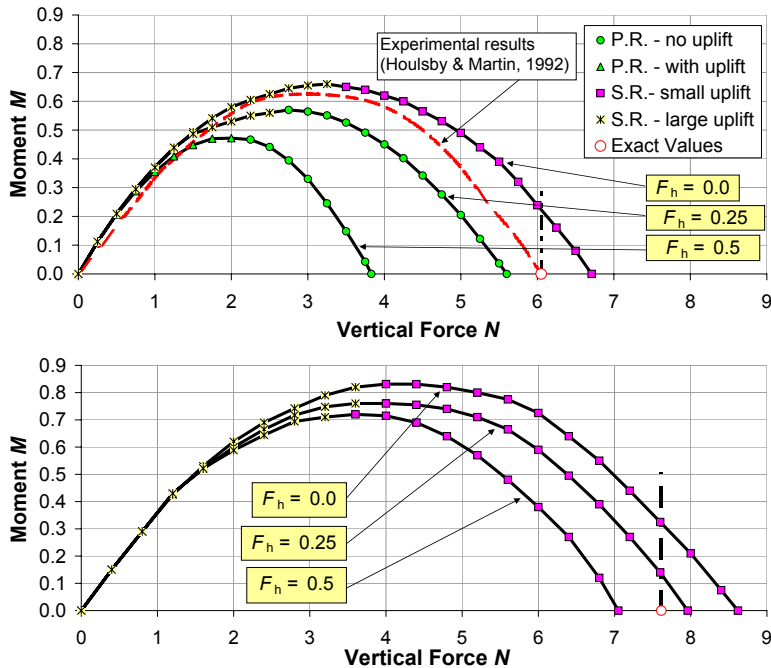
Figure 10. Interaction diagram ($\tilde{N}$, $\tilde{V} = 0$, $\tilde{M}$, $\tilde{F}_h$) for $\tilde{k} = 0$ (top) and $\tilde{k} = 1$ (bottom), and experimental results by Houlsby and Martin [1993]. Tresca criterion with zero tension cut-off.

Conclusion

Seismic actions must now often be taken into account when designing private or industrial buildings or structures such as bridges, dams, nuclear plants, etc. We have briefly outlined how such a problem can be thoroughly studied from the theoretical point of view through the yield design approach up to the writing of new international design codes. For this purpose it is necessary that the rationale of the yield design theory be thoroughly understood since most (not to say all) equations that are used in such codes are obtained through the external approach, either explicitly or implicitly. To this extent the yield design theory is a corner stone of ultimate limit state design (ULSD).

References

[Chatzigogos 2007] C. T. Chatzigogos, *Comportement sismique des fondations superficielles: vers la prise en compte d'un critère de performance dans la conception*, Ph.D. thesis, École Polytechnique Palaiseau, Palaiseau, France, 2007, Available at http://www.imprimerie.polytechnique.fr/Theses/Files/Chatzigogos.pdf.

[Chatzigogos et al. 2007] C. T. Chatzigogos, A. Pecker, and J. Salençon, "Seismic bearing capacity of a circular footing on a heterogeneous cohesive soil", *Soils Found.* **47**:4 (2007), 783–787.

[Coleman and Li 1996] T. F. Coleman and Y. Li, "An interior trust region approach for nonlinear minimization subject to bounds", *SIAM J. Optim.* **6**:2 (1996), 418–445.

[Eurocode 1998] "Calcul des structures pour leur résistance aux séismes", EUROCODE 8, Commission Europénne de Normalisation, 1998. Partie 5.

[Fishman et al. 2003] K. L. Fishman, R. Richards Jr., and D. Yao, "Inclination factors for seismic bearing capacity", *J. Geotech. Geoenviron.* **129**:9 (2003), 861–865.

[Green 1954] A. P. Green, "The plastic yielding of metal junctions due to combined shear and pressure", *J. Mech. Phys. Solids* **2**:3 (1954), 197–211.

[Hansen 1953] J. B. Hansen, *Earth pressure calculation: application of a new theory of rupture to the calculation and design of retaining walls, anchor slabs, free sheet walls, anchored sheet walls, fixed sheet walls, braced walls, double sheet walls and cellular cofferdams*, Danish Technical Press — Institution of Danish Civil Engineers, Copenhagen, 1953.

[Houlsby and Martin 1993] G. T. Houlsby and C. M. Martin, "Modelling of the behaviour of foundations of jack-up units on clay", pp. 339–358 in *Predictive soil mechanics*, edited by G. T. Houlsby and A. N. Schofield, Thomas Telford, London, 1993.

[Knappett et al. 2006] J. A. Knappett, S. K. Haigh, and S. P. G. Madabhushi, "Mechanisms of failure for shallow foundations under earthquake loading", *Soil Dyn. Earthq. Eng.* **26**:2-4 (2006), 91–102.

[Mendoza and Auvinet 1988] M. J. Mendoza and G. Auvinet, "The Mexico earthquake of September 19, 1985 — behavior of building foundations in Mexico City", *Earthq. Spect.* **4**:4 (1988), 835–852.

[Paolucci and Pecker 1997a] R. Paolucci and A. Pecker, "Soil inertia effects on the bearing capacity of rectangular foundations on cohesive soils", *Eng. Struct.* **19**:8 (1997), 637–643.

[Paolucci and Pecker 1997b] R. Paolucci and A. Pecker, "Seismic bearing capacity of shallow strip foundations on dry soils", *Soils Found.* **37**:3 (1997), 95–105.

[Pecker and Salençon 1991] A. Pecker and J. Salençon, "Seismic bearing capacity of shallow strip foundations on clay soils", pp. 287–304 in *Proceedings of International Workshop on Seismology and Earthquake Engineering* (Mexico City), CENAPRED Mexico City, 1991.

[Puzrin and Randolph 2003a] A. M. Puzrin and M. F. Randolph, "Generalized framework for three-dimensional upper bound limit analysis in a tresca material", *J. Appl. Mech.* (*Trans. ASME*) **70**:1 (2003), 91–100.

[Puzrin and Randolph 2003b] A. M. Puzrin and M. F. Randolph, "New planar velocity fields for upper bound limit analysis", *Int. J. Solids Struct.* **40**:13-14 (2003), 3603–3619.

[Richards et al. 1993] R. J. Richards, D. G. Elms, and M. Budhu, "Seismic bearing capacity and settlements of foundations", *J. Geotech. Eng. ASCE* **119**:4 (1993), 662–674.

[Salençon 1983] J. Salençon, *Calcul à la rupture et analyse limite*, Presses de l'E.N.P.C., Paris, 1983.

[Salençon 1990] J. Salençon, "An introduction to the yield design theory and its applications to soil mechanics", *Eur. J. Mech. A Solid.* **9**:5 (1990), 477–500.

[Salençon 1994] J. Salençon, "Approche théorique du calcul aux états limites ultimes", pp. 701–722 in *Les grands systèmes des sciences et de la technologie*, edited by J.-L. L. J. Horowitz and, Masson, Paris, 1994.

[Salençon 2001] J. Salençon, *Handbook of continuum mechanics: general concepts — thermoelasticity*, Springer, Berlin, 2001.

[Salençon 2002] J. Salençon, *De l'élastoplasticité au calcul à la rupture*, Éditions de l'École Polytechnique, Palaiseau, 2002.

[Salençon and Matar 1982] J. Salençon and M. Matar, "Capacité portante des fondations superficielles circulaires", *J. Mec. Theor. Appl.* **1**:2 (1982), 237–267.

[Salençon and Pecker 1995a] J. Salençon and A. Pecker, "Ultimate bearing capacity of shallow foundations under inclined and eccentric loads, I: purely cohesive soil", *Eur. J. Mech. A Solid.* **14**:3 (1995), 349–375.

[Salençon and Pecker 1995b] J. Salençon and A. Pecker, "Ultimate bearing capacity of shallow foundations under inclined and eccentric loads, II: purely cohesive soil without tensile strength", *Eur. J. Mech. A Solid.* **14**:3 (1995), 377–396.

[Sarma and Iossifelis 1990] S. K. Sarma and I. S. Iossifelis, "Seismic bearing capacity factors of shallow strip footings", *Géotechnique* **40** (1990), 265–273.

[Sekiguchi and Kobayashi 1997] H. Sekiguchi and S. Kobayashi, "Limit analysis of bearing capacity for a circular footing subjected to eccentric loadings", pp. 1029–1032 in *Proceedings of the 14th International Conference on Soil Mechanics and Foundation Engineering - ICSMFE* (Hambourg, 1997), vol. 2, Balkema, Rotterdam, 1997.

[Zeng and Steedman 1998] X. Zeng and R. S. Steedman, "Bearing capacity failure of shallow foundations in earthquakes", *Géotechnique* **48**:2 (1998), 235–256.

JEAN SALENÇON: salencon@lms.polytechnique.fr
Laboratoire de Mécanique des Solides, UMR 7649, École Polytechnique, 91128 Palaiseau Cedex, France

CHARISIS THEODOROU CHATZIGOGOS: charisis.chatzigogos@wanadoo.fr
Laboratoire de Mécanique des Solides, UMR 7649, École Polytechnique, 91128 Palaiseau Cedex, France

ALAIN PECKER: pecker@lms.polytechnique.fr
Geodynamique et Structure, 157 rue des Blains, 92220 Bagneux, France